World Journal of Urology (2025) 43:37
https://doi.org/10.1007/s00345-024-05344-z

RESEARCH

Using three-dimensional virtual imaging of renal masses to improve prediction of robotic-assisted partial nephrectomy Tetrafecta with SPARE score

HaoXiang Huang[1] · Bohong Chen[1] · Cong Feng[1] · Wei Chen[2] · Dapeng Wu[3]

Received: 23 June 2024 / Accepted: 25 October 2024

Abstract

Objective To improve the predictability of outcomes in robotic-assisted partial nephrectomy, we utilized three-dimensional virtual imaging for SPARE nephrometry scoring. We compared this method with a conventional two-dimensional scoring system to determine whether 3D virtual images offer enhanced predictive accuracy for Tetrafecta outcomes.

Methods We retrospectively collected basic information, demographic data, and perioperative indices from patients who underwent robot-assisted partial nephrectomy for renal masses at the Department of Urology, First Affiliated Hospital of Xi'an Jiaotong University. A three-dimensional visualization system (IPS system, Yorktal) was employed to reconstruct the patients' imaging data using AI-based automatic segmentation, resulting in a three-dimensional visualization model (3DVM). This model was then imported into the virtual surgical planning software (Touch Viewer System, Yorktal) for automatic measurement of the SPARE score. Tetrafecta was defined as a warm ischemic time (WIT) of less than 25 min, negative surgical margins, absence of major perioperative complications, and no decline in postoperative renal function. The receiver operating characteristic (ROC) curve was utilized to evaluate the sensitivity and specificity of the SPARE score.

Results A total of 141 patients were included in this study, with a mean age of 55.6 ± 11.14 years and a mean tumor size of 3.5 ± 1.2 cm. All variables, except for estimated blood loss (EBL) (Coefficient = 0.056, 0.035; P = 0.514, 0.685), showed significant correlation with the SPARE score when comparing CT and 3D virtual models (Tetrafecta: Coefficient = 0.408, 0.56; P < 0.001, < 0.001; WIT: Coefficient = 0.340, 0.237; P < 0.001, 0.007; ΔeGFR: Coefficient = 0.212, 0.257; P = 0.012, 0.002). The area under the curve (AUC) values from the ROC curves indicated that the 3D virtual model group had significantly better performance than the 2D image group for the SPARE score. However, there was no significant difference in the ROC curves for the SPARE complexity category between the two imaging modalities (AUC for SPARE category with 3DVM = 0.658 vs. AUC for SPARE category with CT = 0.643, P = 0.59; AUC for SPARE score with 3DVM = 0.854 vs. AUC for SPARE score with CT = 0.755, P < 0.001).

Conclusions The SPARE score combined with 3DVM has a more accurate predictive ability for Tetrafecta of RAPN compared to the traditional 2D SPARE score.

Keywords Robot-assisted partial nephrectomy · Nephrometry scores · 3D virtual imaging

Introduction

Robot-assisted partial nephrectomy has become a mainstream surgical procedure for resection of T1 renal masses due to its minimally invasive advantages [1,2]. Preoperative evaluation of the masses and renal morphology plays a key role in guiding the surgery.Currently, the most commonly used nephrometry modalities are PADUA score, RENAL score, and so on. They can provide several assessment indicators to describe the impact of tumor size and location on surgery and evaluate the difficulty of surgery

✉ Dapeng Wu
wudapeng@xjtufh.edu.cn

Wei Chen
chenwei_urology@xjtufh.edu.cn

[1] Department of Urology, The First Affiliated Hospital of Xi'an Jiaotong University, Xi'an 710061, China

[2] Department of Urology, The First Affiliated Hospital of Xi'an Jiaotong University, Xi'an 710061, Shaanxi, China

[3] Department of Urology, The First Affiliated Hospital of Xi'an Jiaotong University, Xi'an 710061, Shaanxi, China

Published online: 19 December 2024

[3,4]. However, these scores are based on two-dimensional (2D) images and are inadequate in predicting postoperative complications [5].

Traditional morphological scoring of renal masses requires surgeons to examine numerous CT scans and "reconstruct" the renal mass on each image mentally to visualize how the mass relates to the parts of the kidney in three dimensions, and then score the mass according to the scoring criteria. Often this process can be highly subjective and suffers from interobserver variability.With the advancement of artificial intelligence algorithms in recent years, we have a better approach for image processing of renal masses. The reconstruction software reduct the scanned images into a three-dimensional model, which is then standardized by computer for evaluation, which can improve the accuracy and objectivity of the scoring [6].

In this study, to enhance the predictability of robotic-assisted partial nephrectomy outcomes, we employed three-dimensional virtual images for SPARE nephrometry scoring [7] and compared them with a conventional two-dimensional scoring system to assess whether 3D virtual images exhibit a more accurate predictive ability for Tetrafecta.

Patients and methods

Study design

We collected clinical data from 141 patients who completed partial nephrectomy at the First Affiliated Hospital of Xi'an Jiaotong University from September 2019 to August 2023, as well as their enhanced CT data and performed 3D reconstruction.All surgical operations are performed by senior chief urologists.The aim of this study was to predict surgical outcomes, and there were no interventions on surgical procedures or patients.Ethical approval from our institutional ethics committee was not required.

Surgical approach

Robot-assisted partial nephrectomy was performed on all patients in this study, with either a transabdominal or retroperitoneal approach based on the mass's location. The renal artery was occluded with laparoscopic artery clamps, and the mass and part of the renal tissue were resected with scissors, creating a wedge resection 0.5–1 cm from the edge of the mass, ensuring the mass was resected intact. The collecting system was closed intermittently with 3–0 absorbable sutures, while the outer renal parenchyma was closed intermittently with 2–0 absorbable sutures.

3D virtual model reconstruction with SPARE scoring

Automatic measurement of SPARE score. A three-dimensional visualization system (IPS system, Yorktal)[8]was applied to reconstruct the patient image data with automatic AI segmentation to obtain three-dimensional visualization images. The reconstructed 3D visualization images were imported into the virtual surgical planning software (Touch Viewer System, Yorktal) for automatic measurement of SPARE score.

SPARE scoring indexes: (1) the longest diameter of the mass; (2) Exophytic rate of the mass; (3) the location of the mass; (4) Whether the mass invades the renal sinus.

SPARE score measurement operation process:

The reconstructed three-dimensional model was imported into the virtual surgical planning software, where it can be rotated, scaled, and displayed with adjustable transparency. The software also allows for automatic measurement of both the long and short diameters, as well as simulation of cutting and other surgical operations. (1) Measurement of short and long diameters: Select and display the mass to be calculated in the 3D view, click on the short and long diameter measurement tool, the system automatically calculates and the results are displayed in the 3D view. (2) Mass convexity: Select and display the mass to be cut in the 3D view, and display the kidney where the mass is located at the same time, click on the surface cutting tool, and draw a closed curve along the edge of the renal parenchyma, the system will automatically generate a plane to divide the mass into two parts, and display the volume and the volume of the percentage of the mass. (3) Position of the mass: Select and display the kidney where the mass is located in the 3D view, and click on the long and short diameters measurement tool to measure the upper edge of the kidney. The longest distance between the upper and lower edges of the kidney will be measured to determine the location of the mass. (4) Whether the mass invades the renal sinus: Select and display the kidney and the mass in the 3D view to determine whether it invades the renal sinus.

All CT scans in this study were performed using high-definition imaging protocols with a slice thickness of 1 mm, conducted on a Philips CT scanner (Philips, Best, The Netherlands) to ensure high-resolution outputs suitable for 3D modeling. We adhere to strict internal quality control procedures, where both radiologists and bioengineers review the images to ensure they meet the necessary standards for clarity and accuracy Fig. 1.

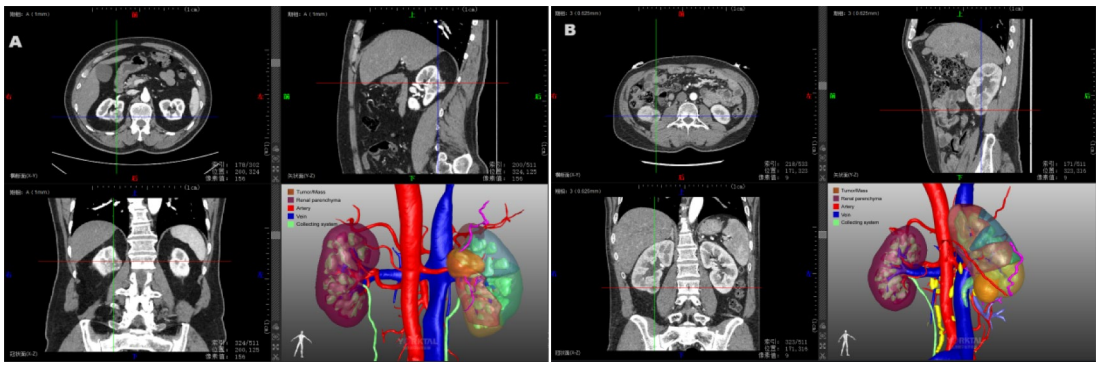

SPARE	Polar location	Exophytic rate	Renal rim	Renal sinus	Tumour size	SPARE	Polar location	Exophytic rate	Renal rim	Renal sinus	Tumour size
2D scan	2	1	1	2	1	2D scan	2	2	1	2	1
3DVM	2	3	2	2	1	3DVM	1	3	2	2	2

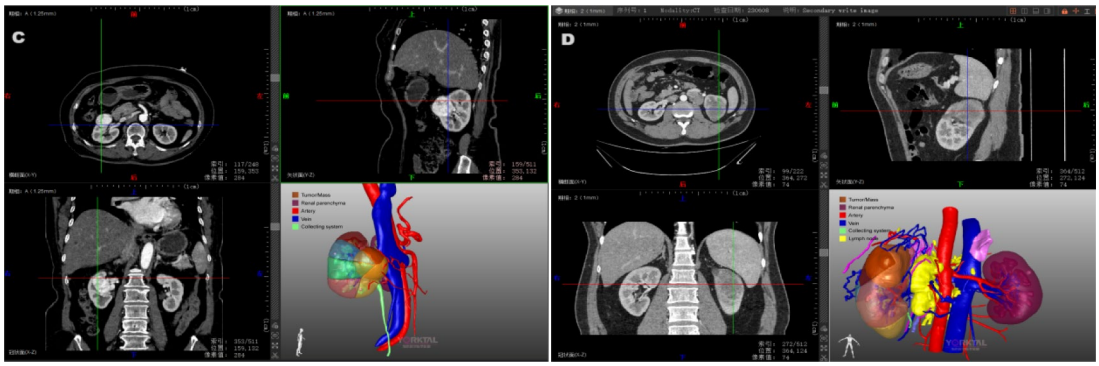

SPARE	Polar location	Exophytic rate	Renal rim	Renal sinus	Tumour size	SPARE	Polar location	Exophytic rate	Renal rim	Renal sinus	Tumour size
2D scan	2	2	2	2	2	2D scan	2	2	1	2	2
3DVM	2	3	2	2	2	3DVM	2	3	2	2	2

Fig. 1 Several cases were used to demonstrate how the SPARE score can be applied to 2D and 3D VMs for assessment, respectively

Data collection

We collected basic information, demographic data(age, sex, body mass index, comorbidities classified according to Charlson's comorbidity index [9] and American Society of Anesthesiologists score(ASA) [10]),perioperative-related markers, pathologic data (the stage according to TNM classification [11] and histology and grading according to the WHO and International Society of Urological Pathology [12] (ISUP) classifications), and postoperative complication data.Clavien-Dindo classification [13] < grade III was considered a mild complication, and ≥ grade III was considered a severe complication. Tetrafecta outcomes were defined as thermal ischemia time (WIT) < 25 min, negative surgical margins, no major perioperative complications, and no reduction in postoperative renal function.SPARE score in 3DVM measured by the engineer and doublech-ecked by an experienced urologist and the 2D group were scored by two single-blinded urologists in previously reported methods [14–16].

Statistical analysis

Mean and standard deviation were used to describe continuous variables. Categorical variables were described using n(%). Student's t-test was used to compare means between the two groups. Spearman's correlation coefficient was used for correlation analysis between continuous variables, while Kendall's correlation coefficient was chosen for correlation analysis between continuous and dichotomous variables.Receiver-operating characteristic curve was used to evaluate the sensitivity and specificity of the SPARE score. The delong test was used to test whether there was a significant difference between two ROC curves. Statistical analysis was performed using SPSS software 25.0 and R 4.3.2.

Results

A total of 141 patients were included in this study. The mean age was 55.6 ± 11.14 years. The mean tumor size was 3.5 ± 1.2 cm. Median body mass index was 24.5 ± 2.9 。 Demographic data and basic clinical information of the 141 patients are summarized in Table 1.

No positive surgical margins was reported, Preoperative eGFR was 101 ± 15.1 ml/min·1.73 m2, Postoperative eGFR was 91.2 ± 17.7 ml/min·1.73 m2, ΔeGFR was 9.8 ± 13.3 ml/min·1.73 m2, Post-operative complications occurred in 20 (14.2%) patients, of whom 9 (6.4%) classified as major complication (Table 2).

We selected five indices of Renal rim, Renal sinus, Tumour size, Exophytic rate, and Polar location.Renal sinus ($P < 0.001$), Tumour size ($P < 0.01$), and Exophytic rate ($P < 0.01$) were significantly different between the significant differences between CT/3DVM groups. In addition, the distributions of SPARE-score and SPARE risk category ($P < 0.001$) based on CT/3DVM were also significantly different (Table 3).

Table 1 Demographic data and basic clinical information of the 141 patients

Variables	PN
No. patients	141
Age	55.6±11.4
Sex	
Male	104 (73.8%)
Female	37 (26.2%)
BMI	24.5±2.9
ASA	
1	4 (2.8%)
2	110 (78%)
3	27 (19.2%)
Tumor location	
Left	67 (47.5%)
Right	74 (52.5%)
Tumor size (cm)	3.5±1.2
Histopathology	
Clear cell	119 (84.4%)
Papillary	6 (4.3%)
Chromophobe	3 (2.1%)
Angiomyolipoma	5 (3.5%)
Oncocytoma	2 (1.4%)
Others	6 (4.3%)
Clinical T stage, n (%)	
T1a	74 (52.5%)
T1b	62 (44%)
T2a	2 (1.4%)
T2b	0
T3	3 (2.1%)

Table 2 Perioperative and pathology-related information

Surgical approach	
Transperitoneal	34(24.1%)
Retroperitoneal	107(75.9%)
Warm ischaemia time, min, mean (SD)	21±5.1
Estimated blood loss, mL, mean (SD)	82.3±140.9
ISUP grade, n (%)	
Grade 1	5(3.5%)
Grade 2	104(73.8)
Grade 3	8(5.7%)
Grade 4	0
Not applicable	24(17%)
Positive surgical margins, n (%)	0
Preoperative eGFR, ml/min·1.73 m2	101±15.1
Postoperative eGFR, ml/min·1.73 m2	91.2±17.7
ΔeGFR, ml/min·1.73 m2	9.8±13.3
Overall complication	20(14.2%)
Major complication	9(6.4%)

Table 4 demonstrates the correlation coefficients and their significance between SPARE score in 2D, SPARE score in 3D and Tetrafecta, WIT, ΔeGFR, EBL respectively. Kendall correlation coefficients were chosen for Tetrafecta, and Spearman correlation coefficients were chosen for the other variables. We found that except for EBL (Cofficient = 0.056, 0.035; P = 0.514, 0.685), the rest of the variables were correlated with SPARE score with CT/3DVM (Tetrafecta: Cofficient = 0.408, 0.56; $P < 0.001$, < 0.001. WIT:Cofficient = 0.340, 0.237; $P < 0.001$, = 0.007. ΔeGFR:Cofficient = 0.212, 0.257; P = 0.012, 0.002) Fig. 2.

We found that the ROC Curve based on the 3DVM imaging group was significantly better than the 2D image group in SPARE score, the AUC values of the ROC curves are significantly better than 2D image group. (AUC for SPARE score with 3DVM = 0.854 vs AUC for SPARE score with CT = 0.755, $P < 0.001$). However, the ROC Curve based on the 3DVM and 2D image group in SPARE complexity category had no significant difference.(AUC for SPARE category with 3DVM = 0.658 vs AUC for SPARE category with CT = 0.643, P = 0.59).

Discussion

In the early stages of partial nephrectomy (PN), limitations in imaging technology resulted in suboptimal surgical outcomes and numerous postoperative complications. However, with the widespread adoption of CT imaging, PN has emerged as the standard approach for resecting T1 stage renal masses [17]. Nephrometry scoring systems,

Table 3 SPARE score frequency distributions

SPARE score frequency	2D	3D	P
Polar location			
Superior/inferior	80 (56.7%)	81 (57.4%)	0.7
Middle	61 (43.3%)	60 (42.6%)	
Exophytic rate			
<50%	75 (53.2%)	52 (36.9%)	0.01
≥50%	53 (36.6%)	65 (46.1%)	
Endophytic	13 (9.2%)	24 (17%)	
Renal rim			
Lateral	82 (58.2%)	89 (63.1%)	0.39
Medial	59 (41.8%)	52 (36.9%)	
Renal sinus			
Not involved	67 (47.5%)	28 (19.9%)	< 0.001
Involved	74 (52.5%)	113 (80.1%)	
Tumour size			
≤4 cm	102 (72.3%)	78 (55.3%)	0.01
4–7 cm	37 (26.2%)	59 (41.8%)	
>7 cm	2 (1.5%)	4 (2.9%)	
SPARE score			
5	0	1 (0.7%)	< 0.001
6	11 (7.8%)	5 (3.5%)	
7	30 (21.3%)	23 (16.3%)	
8	42 (29.8%)	28 (19.9%)	
9	35 (24.8%)	43 (30.6%)	
10	18 (12.8%)	35 (24.8%)	
11	5 (3.5%)	5 (3.5%)	
12	0	1 (0.7%)	
SPARE risk category			
Low risk	11 (7.8%)	6 (4.3%)	< 0.001
Intermediate risk	107 (75.9%)	94 (66.7%)	
High risk	23 (16.3%)	41 (29.1%)	

Table 4 Correlation between SPARE score and Tetrafecta, WIT, ΔeGFR, EBL respectively

	SPARE score in 2D		SPARE score in 3D	
	Correlation Coefficient	P	Correlation Coefficient	P
Tetrafecta	0.408	< 0.001	0.567	< 0.001
WIT	0.340	< 0.001	0.237	0.007
ΔeGFR	0.212	0.012	0.257	0.002
EBL	0.056	0.514	0.035	0.685

such as RENAL and PADUA, were developed to evaluate renal masses [3,4]. However, these scores, based on CT plain images, fall short in predicting postoperative complications [5]. The advent of 3D imaging and modeling technology has revolutionized this field [18,19]. CT 3D visualization technology provides a clear representation of the spatial anatomical relationships between tissues, automatically measures relevant parameters of target tissues, and assists in precision surgery [20,21]. Consequently, we propose using the 3DVM SPARE scoring system for evaluating renal masses, aiming to enhance the understanding of renal mass morphology and improve the prediction rate of postoperative complications and the PN tetrafecta.

Tumor diameter is a crucial factor in several classic nephrometry scoring systems, reflecting its relationship with the difficulty of partial nephrectomy (PN) and patient prognosis. Larger tumors typically indicate a greater volume of kidney tissue that needs to be resected. Previous studies have demonstrated a correlation between renal mass diameter and long-term renal function after PN. However, this correlation seems less reliable when the tumor exophytic rate is high [22]. Recent studies suggest that long-term renal function after PN depends on the number of normal nephrons preserved post-surgery [23,24]. The more endogenous the mass, the more nephrons are affected for the same diameter, making the mass exophytic rate a critical indicator [25]. However, assessing the exophytic rate using CT plain images is variable due to subjective interpretation by different surgeons [26]. In this study, the maximum diameter and exophytic rate of the mass were automatically calculated using a three-dimensional visualization system (IPS system, Yorktal), eliminating inter-observer variability and enhancing the score's reliability.

The location of the mass significantly impacts PN. For instance, resecting a mass located in the lower pole of the kidney via a retroperitoneal approach poses greater suturing challenges than resecting a mass in the upper pole due to the laparoscope's operational angle. Despite the multiple maneuver angles possible in RAPN, surgeons still face severe complications, such as bleeding and urinary fistula, for masses invading the renal sinus or near the renal hilum [27]. Considering surgical margin [28], the anatomical relationship of the mass to the renal vasculature and collecting system is crucial. This study found a significant correlation between the score and WIT and ΔeGFR, indicating that higher scores reflect a closer relationship between the mass and the renal vascular and collecting system, correlating with surgical difficulty and patient prognosis. The predictive ability for the tetrafecta was significantly different between scores based on CT scans and those based on 3DVM, suggesting that 3DVM enables surgeons to more intuitively understand the anatomical relationship between the mass and critical kidney structures, allowing for more appropriate and precise surgical strategies.

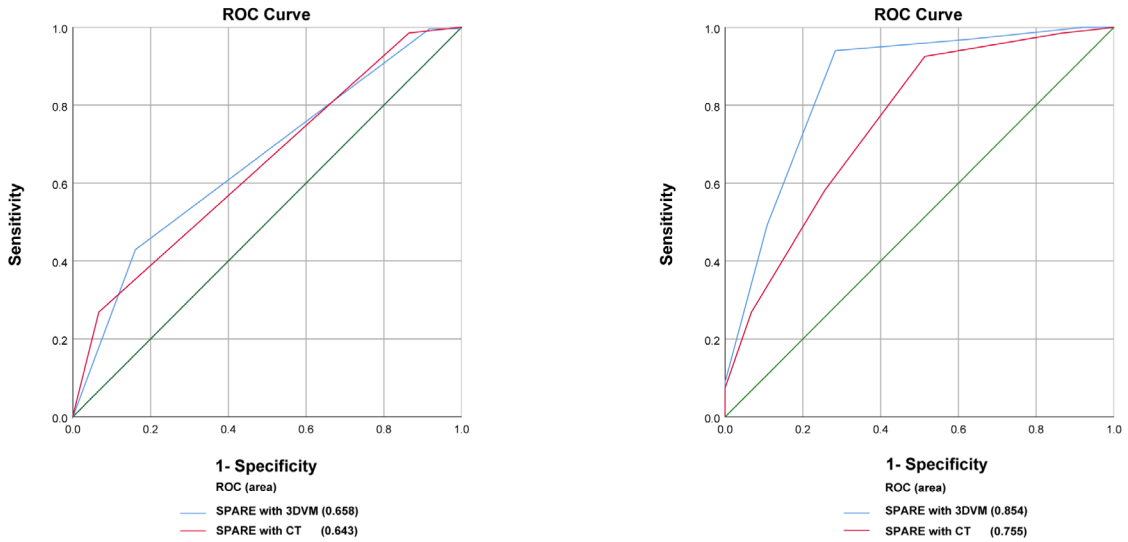

	Area	Standard Error	Asymptotic Significance	95% Wald Confidence Limits	Delong test
Complexity category					
SPARE With 3DVM	0.658	0.046	0.001	0.568-0.748	P=0.59
SPARE With CT	0.643	0.046	0.003	0.552-0.734	
Score					
SPARE With 3DVM	0.854	0.033	0.001	0.79-0.917	P＜0.001
SPARE With CT	0.755	0.04	0.001	0.677-0.834	

Fig. 2 Receiver-operating characteristic (ROC) curve analysis of Tetrafecta. **A** ROC curve analysis of Tetrafecta considering the SAPRE complexity categories evaluated via three-dimensional virtual models (3D VMs) and two-dimensional (2D) CT standard imaging(2D SAPRE complexity category: red line; 3D SAPRE complexity category: blue line). **B** ROC curve analysis of Tetrafecta considering the SPARE score evaluated via 3D VMs and 2D CT standard imaging (2D SAPRE score: red line; 3D SAPRE score: blue line;)

There are some limitations to this study. First, most of the renal masses in the patients included in this study were stage T1, which does not ensure that the conclusions we drew are applicable in stage T2 and more complex renal masses. Second, 3DVM is not yet fully available in the clinic, which requires surgeons to use specialized software for evaluation. Third, this study was conducted in a single high-volume referring center, which is not representative of what may occur in different healthcare settings.

Conclusion

Due to the ability to visualize the spatial anatomical relationship between tissues and automatically measure the relevant parameters of the target tissues, the SPARE score combined with 3DVM has a more accurate predictive ability for Tetrafecta of RAPN compared to the traditional 2D SPARE score.

Author contributions Project development： DPW, WC. Surgery: DPW. Data Collection: HXH, BHC, CF. Data analysis: HXH,BHC. Manuscript writing: XH. All authors reviewed the manuscript.

Funding This study was supported by the XJTU1AF-CRF-2020-018 grant and the Natural Science Basic Research Plan of Shaanxi Province, project number 2022JQ-892.

Data availability No datasets were generated or analysed during the current study. The data that support the findings of this study are available on request from the corresponding author.

Declarations

Conflict of interest The authors declare no competing interests.

References

1. Ljungberg B, Albiges L, Abu-Ghanem Y et al (2022) European Association of Urology Guidelines on Renal Cell Carcinoma: The 2022 Update. Eur Urol 82(4):399–410
2. Choi JE, You JH, Kim DK, Rha KH, Lee SH (2015) Comparison of perioperative outcomes between robotic and laparoscopic partial nephrectomy: a systematic review and meta-analysis. Eur Urol 67(5):891–901
3. Ficarra V, Novara G, Secco S et al (2009) Preoperative aspects and dimensions used for an anatomical (PADUA) classification of renal tumours in patients who are candidates for nephron-sparing surgery. Eur Urol 56(5):786–793
4. Kutikov A, Uzzo RG (2009) The R.E.N.A.L. nephrometry score: a comprehensive standardized system for quantitating renal tumor size, location and depth. J Urol 182:844–853
5. Hew MN, Baseskioglu B, Barwari K et al (2011) Critical appraisal of the PADUA classification and assessment of the R.E.N.A.L nephrometry score in patients undergoing partial nephrectomy. J Urol 186(1):42–46
6. Porpiglia F, Amparore D, Checcucci E et al (2019) Three-dimensional virtual imaging of renal tumours: a new tool to improve the accuracy of nephrometry scores. BJU Int 124(6):945–954. https://doi.org/10.1111/bju.14894
7. Checcucci E, Amparore D, Fiori C et al (2020) 3D imaging applications for robotic urologic surgery: an ESUT YAUWP review. World J Urol 38(4):869–881. https://doi.org/10.1007/s00345-019-02922-4
8. Li XF, Peng YJ, Yu XT, et al (2021) Beijing Da Xue Xue Bao Yi Xue Ban 53(3):613-622
9. Charlson ME, Pompei P, Ales KL, MacKenzie CR (1987) A new method of classifying prognostic comorbidity in longitudinal studies: development and validation. J Chronic Dis 40:373–383
10. Ament R (1979) Origin of the ASA classification. Anesthesiology 51:179
11. Sobin LH, Gospodariwicz M, Wittekind C (eds) (2009) TNM Classification of Malignant Tumors. UICC International Union Against Cancer, 7th edn. Wiley-Blackwell, 255.
12. Moch H (2016) WHO-ISUP-graduierungssystem für nierenkarzinome. Pathologe 37:355–360
13. Dindo D, Demartines N, Clavien PA (2004) Classification of surgical complications: a new proposal with evaluation in a cohort of 6336 patients and results of a survey. Ann Surg 240:205–210
14. Kutikov A, Uzzo RG (2009) The R.E.N.A.L. nephrometry score: a comprehensive standardized system for quantitating renal tumor size, location, and depth. J Urol 182:844–853
15. Ficarra V, Novara G, Secco S et al (2009) Preoperative aspects and dimensions used for an anatomical (PADUA) classification of renal tumors in patients who are candidates for nephron-sparing surgery. Eur Urol 56:786–793
16. Simmons MN, Hillyer SP, Lee BH et al (2012) Diameter-axial-polar nephrometry: integration and optimization of R.E.N.A.L. and centrality index scoring systems. J Urol 188:384–390
17. Campbell SC, Novick AC, Belldegrun A et al (2009) Guideline for management of the clinical T1 renal mass. J Urol 182(4):1271–1279
18 Piana A, Amparore D, Sica M et al (2024) Automatic 3D augmented-reality robot-assisted partial nephrectomy using machine learning: our pioneer experience. Cancers (Basel). 16(5):1047
19. Piramide F, Kowalewski KF, Cacciamani G et al (2022) Three-dimensional model-assisted minimally invasive partial nephrectomy: a systematic review with meta-analysis of comparative studies. Eur Urol Oncol 5(6):640–650. https://doi.org/10.1016/j.euo.2022.09.003
20. Cartiaux O, Paul L, Francq BG, Banse X, Docquier PL (2014) Improved accuracy with 3D planning and patient-specific instruments during simulated pelvic bone tumor surgery. Ann Biomed Eng 42(1):205–213
21. Di Dio M, Barbuto S, Bisegna C et al (2023) Artificial intelligence-based hyper accuracy three-dimensional (HA3D®) models in surgical planning of challenging robotic nephron-sparing surgery: a case report and snapshot of the state-of-the-art with possible future implications. Diagnostics (Basel) 13(14):2320
22. Zhang ZY, Pan X, Fan Y et al (2019) DDD score for renal tumor: An intuitive and comprehensive anatomical scoring system to access the outcomes of retroperitoneal laparoscopic partial nephrectomy. Int J Urol 26(4):451–456
23. Bertolo R, Fiori C, Piramide F et al (2018) Assessment of the relationship between renal volume and renal function after minimally-invasive partial nephrectomy: the role of computed tomography and nuclear renal scan. Minerva Urol Nefrol 70(5):509–517
24. Antonelli A, Minervini A, Sandri M et al (2018) Below safety limits, every unit of glomerular filtration rate counts: assessing the relationship between renal function and cancer-specific mortality in renal cell carcinoma. Eur Urol 74(5):661–667
25. Leslie S, Gill IS, de Castro Abreu AL et al (2014) Renal tumor contact surface area: a novel parameter for predicting complexity and outcomes of partial nephrectomy. Eur Urol 66:884–893
26. Wadle J, Hetjens S, Winter J et al (2018) Nephrometry scores: the effect of imaging on routine read-out and prediction of outcome of nephron-sparing surgery. Anticancer Res 38(5):3037–3041
27. Wang D, Zhang B, Yuan X, Zhang X, Liu C (2015) Preoperative planning and real-time assisted navigation by three-dimensional individual digital model in partial nephrectomy with three-dimensional laparoscopic system. Int J Comput Assist Radiol Surg 10(9):1461–1468
28. Laganosky DD, Filson CP, Master VA (2017) Surgical margins in nephron-sparing surgery for renal cell carcinoma. Curr Urol Rep 18:8